WILEY | Hindawi

Research Article

The Occurrence of Adsorbed Tight Oil and Its Effect on Porosity and Permeability Reduction of Triassic Lacustrine Sandstone Reservoir

Qianshan Zhou [ID],[1,2] **Xiaotian Li** [ID],[3] **Zhaoming Qian** [ID],[4,5] **Guojun Chen** [ID],[1,2] **Chengfu Lyu** [ID],[1,2] **Xiaofeng Ma** [ID],[1,2] **and Chao Li** [ID][1,2]

[1]*Northwest Institute of Eco-Environment and Resources, Chinese Academy of Sciences, Lanzhou 730000, China*
[2]*Key Laboratory of Petroleum Resources Research, Gansu Province, Lanzhou 730000, China*
[3]*Exploration and Development Research Institute of PetroChina Changqing Oilfield Company, Xian, 710018, China*
[4]*Daye Nonferrous Metals Co., Ltd., Huangshi 435232, China*
[5]*Kambove Mining SAS, Katanga Likasi, Congo*

Correspondence should be addressed to Chao Li; lichaomails@lzb.ac.cn

The adsorption of crude oil in the tight sandstone reservoir is significant. Occurrence states of adsorbed tight oil and its pore and throat reduction effect are two significant directions in tight oil exploration and development. In this paper, the occurrence state of adsorbed tight oil and its porosity and permeability reduction effect is systematically analyzed based on a detailed description and discussion of occurrence space, states, changes of porosity and permeability, and its controlling factors. Five occurrence states are recognized based on the differences in spatial location and morphology of adsorbed tight oil. Adsorbed oil is distributed in all kinds of reservoir spaces and primarily concentrated in the pore – throat radius $< 0.25\,\mu$m. The distribution characteristics of reservoir spaces control the occurrence states of adsorbed tight oil. The emulsion form, cluster form, throat form, thin film form, and isolation form are mainly stored in intergranular pores, feldspar dissolved pores, throats, the surface of minerals, and intercrystalline pores, respectively. The massive development of quartz, feldspar, and illite is conducive to the distribution of emulsion form, cluster form, and the throat form of tight oil, while the abundance of clay, especially chlorite, controls the distribution of the thin film form and isolated form of tight oil. The adsorption of tight oil causes clogging in the pore network, resulting in reservoir damage. The adsorption of tight oil in the reservoir leads to increased reservoir density by $0.290\,\text{g/cm}^3$ and the reduction of porosity and permeability by 3.14% and $0.321 \times 10^{-3}\,\mu\text{m}^2$, respectively. And the damage of adsorbed oil to permeability (30.79%) is more severe than that of porosity (19.96%). The effect of pore and throat reduction is more evident in reservoirs with higher content of quartz and feldspar. However, the strong adsorption of clay makes it difficult to separate the tight oil adsorbed on its surface. The nature of adsorbed oil in different occurrence states also can determine the separation efficiency in the extraction process. The adsorbed tight oil with emulsion, cluster, and throat forms is easier to desorb than the isolation and thin film forms. The research results can provide a basis for analyzing the occurrence characteristics and reasonably formulating the development method of tight oil. In addition, it can even provide a new understanding and basis for the densification process of reservoir permeability under different conditions.

1. Introduction

With the successful exploration and development of tight oil in North America, tight oil has become a new hotspot of energy replacement in global energy study. As the large-scale commercial exploitation of tight oil from Eagle Ford, Bakken, Niobrara, and Wolfcamp has been successfully achieved, unconventional oil and gas development

revolution has been triggered in the United States and worldwide [1–13]. The occurrence morphology of tight oil in porous media of tight reservoir can mainly be divided into two categories. One is free tight oil, and the other is adsorbed tight oil. Free tight oil occurs in larger pores and can flow freely under lower pressure. And adsorbed tight oil occurs on the edges of large pores or occurs in micropore, which cannot generally flow due to capillary force and viscous force [14–16].

The differences in chemical composition and structural properties of adsorbates and adsorbents control the different adsorption behavior of crude oil on different material surfaces [17–21]. The adsorption capacity and adsorption process of asphaltene on different material surfaces have been experimented with, such as glass, silica, gold, alumina, iron, zeolite, polymers, and metal oxides surface [17, 22–27]. The adsorption process of asphaltene on the surface of mineral particles has also been studied [21, 28–30]. They all stated that the adsorption process is controlled by the properties of adsorbents themselves and by the properties of adsorbates—however, few related studies on the occurrence state of tight oil in the reservoir. By using micro-nano CT scanning technology, the micro-occurrence states of tight oil of Chang 7 Member of Triassic Yanchang Formation in Ordos Basin were divided into six types (include thin film form, cluster form, throat form, emulsion form, particle form and isolation form) [31]. Using the Environmental Scanning Electron Microscope to characterize tight oil's occurrence morphology in micro- and nanopores of tight sands in Member 4 of Cretaceous Quantou Formation divided the occurrence morphology of tight oil into two primary forms (oil film and oil droplet) [32]. However, these studies mainly focus on the adsorption capacity of asphaltene on different material surfaces or the occurrence state of tight oil in tight sandstone, without considering the adsorption of tight oil under actual geological conditions. And there are no reports on pore structures with occurrence morphology of adsorbed tight oil.

China's tight oil reservoirs are predominately lacustrine deposited. And several basins have been reported to hold large-scale commercial tight oil resources, such as the Songliao, Ordos, Sichuan, Tuha and Santanghu, Junggar, Qaidam, and Bohai Bay basins [33–37]. In the Ordos Basin, there is a massive amount of tight oil resources, and the geological resources of the 6th, 7th, and 8th members of the Yanchang Formation are 12.13×10^8, 9.00×10^8, and 9.50×10^8 t, respectively [38]. However, many researchers have made significant achievements in exploration and development and a series of geological theories in Ordos Basin tight sandstone reservoirs [33–35]. However, little research is available on the microscopic occurrence characteristics and the tight oil absorbed in different pore scales. Although the tight oil resources in Ordos Basin are enormous, the adsorbed tight oil as a potential resource for EOR should not be ignored. The adsorbed layer of tight oil on reservoir pore and mineral particle surface reduces reservoir porosity and permeability and affects oil and gas migration and exploitation. Especially for tight sandstone reservoirs, the effect of pore reduction and throat reduction is noticeable, even up to about 10%~30% [39]. Therefore, it is urgent to study the effect of adsorbed tight oil on reservoir reconstruction.

In this study, Chang 8 tight oil sandstone reservoir of Yanchang Formation in the Huaqing area of Ordos Basin is selected as the research object, based on the mineral analysis, physical property testing, pore structure division, and occurrence morphology of adsorbed tight oil, combined with Soxhlet extraction method, emphasis on the analysis of the occurrence of adsorbed tight oil in actual geological samples, and the adsorption of mineral particles on the tight oil and the adsorbed tight oil effect on reservoir modification. A suitable development process can select according to the different occurrence forms of adsorbed tight oil by analyzing the occurrence form of adsorbed tight oil and its influence on reservoir reconstruction, to explore the method to improve the conversion efficiency from adsorbed tight oil to free tight oil.

2. Geological Setting

The Ordos Basin, the second largest basin in China, belongs to the craton marginal depression basin, is located in the western region of the North China Platform (Figure 1). Ordos Basin is a large depression basin formed by gravity load compensation, separated from the continental margin tectonic domains of northern China only after the docking and assembling of Siberia-Mongolia plate and North China-Tarim continental margin in the late Hercynian period and the Indosinian movement. According to its structural features, the Ordos Basin can divide into six tectonic units: the Western thrust belt, Tianhuan depression, Yimeng uplift, Weibei uplift, and Jinxi fault-fold belt, and Yishan slope [40]. The collision process in the Ordos Basin has the characteristics of fluctuation. Early in the Yanchang Formation, Indosinian tectonic activity was weak. From the end of Chang 8, the Indosinian tectonic cycle intensified, and fault activities and event deposits were frequent. Affected by the intense collision and rapid uplift of the Qinling orogenic belt, the lake basin area expanded rapidly. The water body deepened, the center of the lake basin moved westward, and the lake basin basement inclined unevenly. After the deposition period of Chang 7, the compressive stress field of the basin changed from north-south to left-lateral shear stress, the intensity of Indosinian movement gradually weakened, and the Erdos block began the filling development stage large inland basins. The whole Yanchang Formation is an asymmetrical dustpan depression with gentle north and steep south and open southeast of the lake basin [14].

Ordos Basin is a relatively independent large-scale inland lake basin, with Qilian Mountains in the West and Qinling Mountains in the south. Under the influence of the Indonesian movement and the stability of stable blocks in North China, Ordos Basin has entered a long-term sedimentary period of a large-scale inland lake basin. The Late Triassic sediments are relatively stable and continuous as
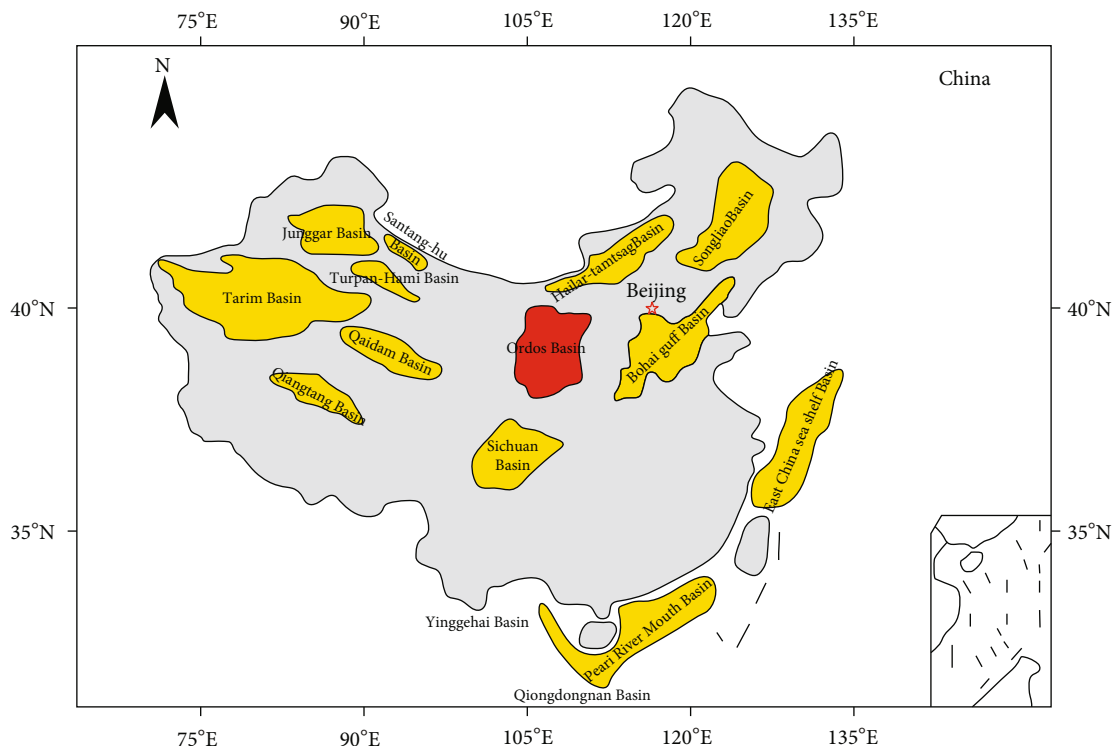
FIGURE 1: Regional overview of the Ordos Basin, China, and the location of the study area.

the whole basin—lacustrine deltas developed in the northeast, northwest, and southwest.

The Yanchang Formation in the Huaqing area has experienced a period from transgressive system to the peak of lake basin development, then to lake basin construction, and gradual shrinkage. During Chang 8 to Chang 6 period, there were several secondary cycles of inflow and recession. Due to channel lateral displacement, hydrodynamic conditions, and provenance, the sandstone and mudstone profiles in the delta front with multichannel, multiestuary bar, and multichannel overlapping are formed provenances of the study area vertically, mainly from northeast and southwest. During the deposition of the Chang 8 reservoir group in the Huaqing area, the basement of the basin continued to subside, and the lacustrine basin was still in the stage of development. The northeast meandering river and the southwest braided river converge in the study area to form a shallow water delta sedimentary system. The study area is mainly in front of the meandering river and braided river delta. During the Chang 8 period, distributary channels, estuary bars, overflow sands, sheet sands, and interdistributary bays were mainly developed, distributed in a circular belt around the lake shoreline [41].

Six tight oil sandstone samples were collected from Chang 8 of the Upper Triassic Yanchang Formation in the Huaqing area. And the administrative region is affiliated with Huachi County and Qingyang County of Gansu province.

3. Samples and Methods

3.1. Samples.
Six samples with suitable oil-bearing properties were selected from Chang 8 reservoir of Yanchang Formation in the Huaqing area, Ordos Basin. All samples were collected from Core pillars with a diameter and length of 40 mm × 25 mm. Moreover, the core samples have experienced field displacement, and it is considered that the remaining tight oil is adsorbed oil.

3.2. Methods and Procedures

3.2.1. Porosity and Permeability.
Pore PDP-200 is an instrument measuring porosity and permeability under overburden pressure. Six samples were tested for helium porosity and nitrogen permeability before and after Soxhlet extraction, respectively, according to China's SY/T 6385-2016 standard.

3.2.2. Fluorescence Thin Sections.
According to the different luminous colors of hydrocarbons and other organic matter in rocks under ultraviolet excitation, the hydrocarbon-bearing properties can be determined by the differences in fluorescent colors, brightness, and luminous sites. The samples before Soxhlet extraction were identified by Nikon 80i three-channel advanced fluorescence microscope, execution according to China's SY/T5614-2011 standard.

3.2.3. High-Pressure Mercury Intrusion (HPMI).
The Autopore IV, 9510 high-pressure automatic mercury injection

TABLE 1: Sample information and rock mineral composition of Chang 8 reservoir.

Sample	Depths (m)	Mineral composition (%)						
		Quartz	Feldspar	Clay	Others	Illite	Chlorite	I/S mixed layer
B455-2-46	2147.87	50.7	39.6	8.6	1.1	28	53	19
B455-2-60	2149.47	50.2	38.0	10.3	1.5	25	58	17
B436-7-33	2192.60	50.3	33.1	12.7	3.9	19	66	25
B436-7-38	2193.20	50.2	34.2	11.8	3.8	14	64	22
B456-6-6	2134.20	50.0	36.3	12.2	1.5	11	75	14
B280-13-3	2213.35	49.8	32.0	13.8	4.4	5	83	12

Others: calcite+dolomite+pyrite; I/S mixed layer: illite and smectite mixed layer.
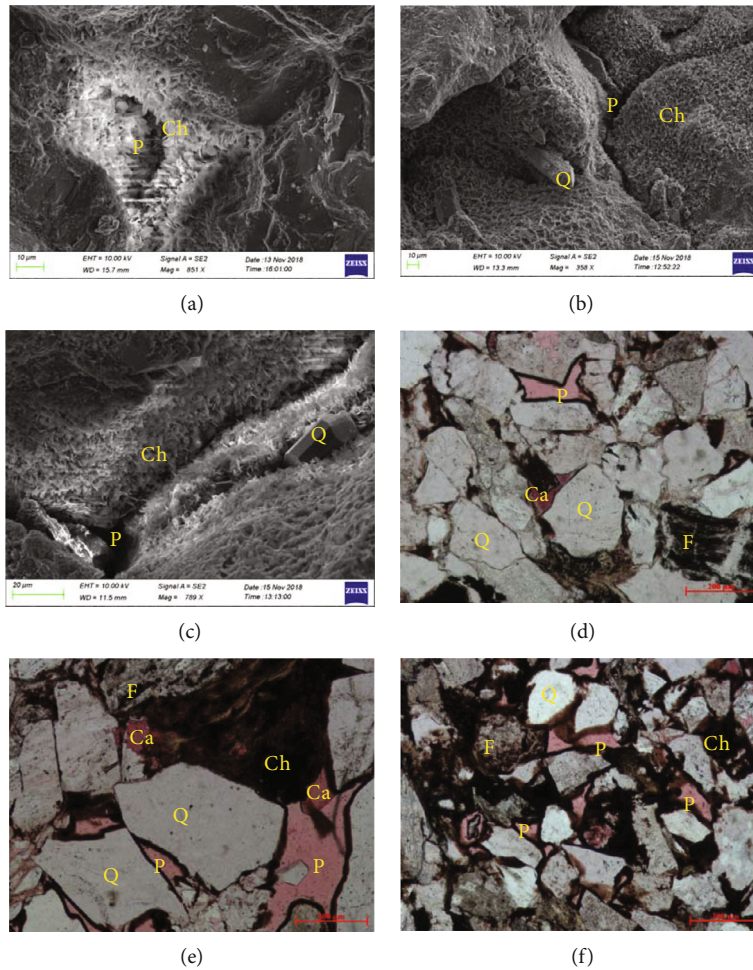

(a)

(b)

(c)

(d)

(e)

(f)

FIGURE 2: Typical pore types found in the tight oil sandstone samples. (a) Residual interparticle pores coated by chlorite (B280-13-3). (b) Chlorite and residual organic matter dominate the residual interparticle pores (B436-7-38). (c) Residual interparticle pores with feldspar dissolution (B455-2-46). (d) Interparticle pore and feldspar dissolved pores (B436-7-33). (e) Interparticle pore and calcite cementation, residual interparticle pores filled with adsorbed organic matter (B455-2-60). (f) The intergranular pore and feldspar dissolved pore filled with adsorbed organic matter (B456-6-6) (Q: quartz; F: feldspar; Ca: calcite; Ch: chlorite; P: pores).

apparatus, was used in this experiment, execution according to the GB/T 21650.1-2008/ISO 15901-1 standard of China after Soxhlet extraction [42, 43]. The test specification of the instrument ranged from 3 nm to 1000 μm, and the volume accuracy of mercury intake and removal was less than 0.1 μm L. The samples were dried for 24 hours after being made into core columns, the test temperature was 17°C,

and the maximum mercury injection pressure can reach 230 MPa.

3.2.4. Field Emission Scanning Electron Microscopy (FE-SEM). Field emission scanning electron microscopy (FE-SEM) uses focused high-energy electron beams to scan the samples, and the surface morphology of the tested samples

TABLE 2: Pore structure parameters of HPMI.

| Samples	Depths (m)	Porosity (%)	Permeability ($\times 10^{-3}$ μm^2)	Average of throat radius (μm)	Sorting coefficient (a.u.)	Displacement pressure (MPa)	Median pressure (MPa)	Efficiency of mercury withdrawal (%)	The most mercury injection saturation (%)
B455-2-46	2147.87	23.57	9.338	3.3	0.38	0.03	1.95	29.63	84.38
B455-2-60	2149.47	16.63	2.901	1.56	0.33	0.05	5.18	33.44	83.1
B436-7-33	2192.60	12.03	0.584	0.275	2.45	0.57	7.82	33	90.47
B436-7-38	2193.20	13.38	0.827	0.42	0.26	0.3	4.9	33.72	85.1
B456-6-6	2134.20	14.35	0.639	0.5	0.24	0.3	4.32	31.76	89.62
B280-13-3	2213.35	13.02	0.244	0.07	1.55	3.72	20.7	34.96	88.119
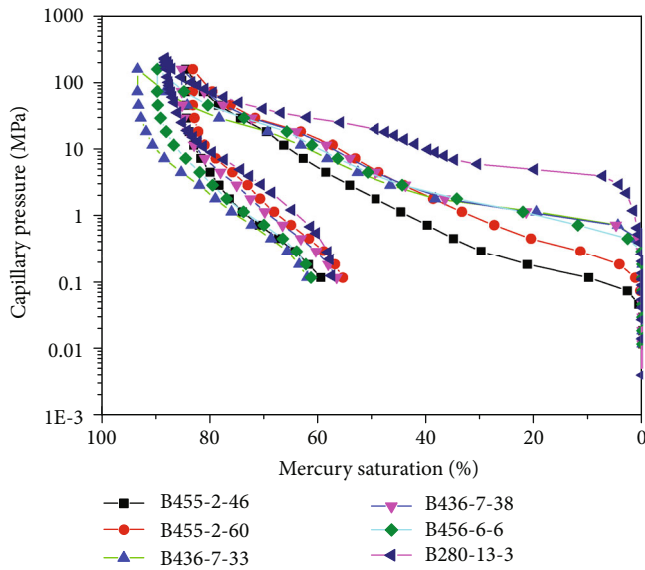
FIGURE 3: Intrusion and extrusion curves of pressure-controlled porosimetry for six samples.

can be observed. The experimental instrument is Merlin Compact field emission scanning electron microscope (Xflash/30), execution according to China's SY/T5614-2011 standard after Soxhlet extraction. The accelerating voltage and resolution were 20 V-30 kV and 1.6 nm, respectively.

3.2.5. X-Ray Diffraction (XRD). X-ray diffraction (XRD) analysis is based on the fact that different minerals have different crystal structures, execution according to the SY/T 5163-2010 standard of China after Soxhlet extraction [43]. The instrument used in this experiment is the Rigaku Ultima type IV X-ray diffractometer of Japan (Cu Kα, $\lambda = 0.154$ nm).

3.2.6. Soxhlet Extraction. Soxhlet extraction can make hydrocarbon substances extracted by pure solvents every time. The samples of tight oil dissolution need to be wrapped with filter paper and placed in the Soxhlet extraction unit to wash oil by continuous extraction for 120 hours, following the SY/T 7313-2016 standard of China. The reagent is prepared by dichloromethane-methanol (volume ratio 93 : 7).

All the experiments above were completed in Lanzhou Oil and Gas Resource Center, Institute of Geology and Geophysics, Chinese Academy of Sciences.

4. Results

4.1. Petrological Characteristics and Pore Types. The Chang 8 member is mainly fine-grained lithic feldspathic sandstone and feldspathic lithic sandstone. Through thin section statistics, it is found that the Chang 8 tight oil sandstone reservoir has the characteristics of low compositional maturity and structural maturity. For instance, XRD reveals (Table 1) that quartz content in diagenetic minerals of Chang 8 reservoir in the Huaqing area is 49.8%~50.75%, with an average of 50.2%. The content of feldspar is 32%~39.6%, with an average of 35.53%, while the clay content is 8.6%~13.8%, with an average of 11.57%, relatively. In addition, the principal clay mineral is chlorite, with relative content ranging from 53% to 83%. The second is illite, with relative content of 5%~28%. Chang 8 Member, tight sandstone in the Huaqing area of Ordos Basin, is a typical reservoir with low porosity, low permeability, ultralow porosity, and permeability. The pore types are various, and the pore sizes vary greatly (Figure 2). The nanomicron scale is distributed widely, and the total surface porosity of the reservoir is less than 3.5%.

The primary pore types are mainly residual interparticle pore, dissolved pore, and intercrystalline pores. The intercrystalline pore in the filling material is characterized by small size, uneven distribution, and poor connectivity, most of which disappear after compaction modification. Only a minor part remains in siltstone with high argillaceous content. The surface porosity of the intercrystalline pore is nearly 0.2%. The residual interparticle pore and the dissolved pore are relatively large, unlike the intercrystalline pore. The shapes of the interparticle pore are mostly triangular or polygonal, and the whole edge is neat, straight, and
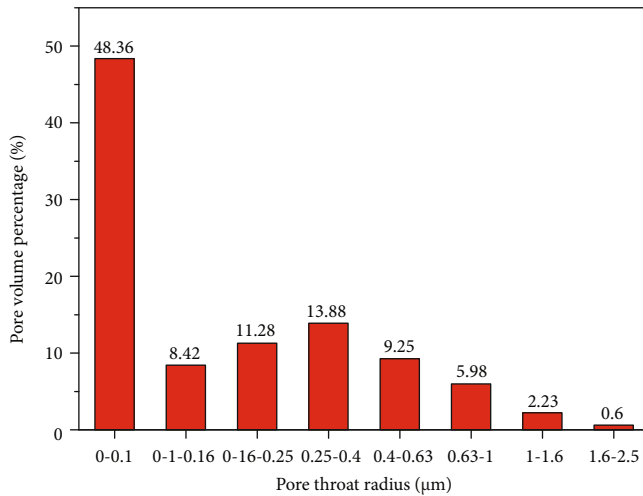
FIGURE 4: Pore size distribution of six samples by HPMI.

enclosed mainly by chlorite film. The dissolution components of interparticle dissolved pore are mainly feldspar and calcite, and the edges of the dissolution particles are harbor-shaped and irregular. The intercrystalline dissolved pore is primarily developed in feldspar, mica, and some debris, and the dissolution usually occurs along the cleavage fracture of feldspar. The surface porosity of residual interparticle pore and dissolved pore is 2.11% and 0.65%, respectively. The diversity of pore types increases the pore throat tortuosity and the complexity of pore structure.

4.2. Pore Throat Structure. The pore structure of the Chang 8 reservoir can be divided into four types: type A, type B, type C, and type D (Table 2 and Figure 3). The displacement pressure is the critical point on the capillary pressure curve where the mercury initially enters the pore throats of the rock, and it corresponds to the maximum pore-throat radius [40]. The displacement pressure of four reservoir types is 0.04 MPa, 0.1 MPa, 0.39 MPa, and 3.72 MPa. The corresponding maximum pore-throat radius of the type A reservoir is 24.513 μm, which is significantly higher than that of type B, type C, and type D reservoirs (14.708 μm, 2.015 μm, and 0.607 μm, respectively).

Median pressure corresponds to the capillary pressure at 50% mercury saturation and the median radius [40]. The median pressure of the type A reservoir is 1.95 MPa on average, which is significantly less than that of type B, type C, and type D reservoirs (5.18 MPa, 5.68 MPa, and 20.7 MPa, respectively). The corresponding average of the pore-throat radius is 3.3 μm, which is much larger than that of type B, type C, and type D reservoirs (1.56 μm, 0.398 μm, and 0.07 μm, respectively). The average displacement pressure is 0.83 MPa, and the average median pressure, average throat radius, and mercury removal efficiency are 7.48 MPa, 1.02 μm, and 32.75%, respectively.

The quantitative pore size analysis is characterized by high-pressure mercury injection. And the pore-throat radius distribution is mainly in the range of 0-0.25 μm, accounting for more than 68.06% of the total pore throat distribution (Figure 4). The pore throat types of Chang 8 reservoir in the study area are mainly thin pore throat and micron pore throat. Chang 8 is a multiscale pore reservoir in the Huaqing area, distributed from nanometer to micrometer pore throat. The micro-nanopore (<2 μm) is the reservoir's leading space capacity for oil and gas.

4.3. The Microoccurrence Characteristics of Adsorbed Tight Oil. Many tight oils' adsorbed layers exist in Chang 8 reservoir, which mainly occurs in the interparticle pore, dissolved pore, and mineral particle surface. Black or brown fluorescence is usually found on the surface of chlorite and iron calcite. Green fluorescent is found in the interparticle pore, dissolved pore, and chlorite surface. Based on the fluorescent thin sections (Figure 5), the occurrence of tight oil in Chang 8 reservoir is divided into five types: the adsorbed tight oil in interparticle pore and feldspar dissolved pore mainly occurring in the form of emulsion and cluster (Figure 5(c)); the adsorbed tight oil mainly occurring in the form of isolation form, mainly in the intercrystalline pore with relatively poor connectivity (Figure 5(d)); the throat tight oil adsorption layer mainly occurring in the form of the long strip and flat (Figure 5(b)), mainly in the throat of the interparticle pore; and the tight oil adsorbed on chlorite and iron calcite surface mainly occurring in the form of thin film and cluster with relatively small adsorption amount (Figure 5(a)).

5. Discussion

5.1. Effect of Adsorbed Tight Oil on the Rock Density Changes. Firstly, six samples were tested for rock density, porosity, and permeability before Soxhlet extraction. Then, Soxhlet extraction is used to dissolve the adsorbed tight oil and later test the rock density, porosity, and permeability after Soxhlet extraction again. The porosity and permeability of reservoirs before and after Soxhlet extraction are compared (Table 3).

The surface of mineral particles and pore throat of the reservoir is filled with adsorbed tight oil (Figure 5), and the relationship between adsorbed tight oil and the rock density of the Chang 8 tight reservoir has been studied (Figure 6). The results show that as the adsorbed tight oil dissolution with the Soxhlet extraction process, the illusion of rock density increases seemly. These results are related to the adsorbed tight oil in reservoir occupies reservoir space such as pore and throat [44]. The rock density of six samples before the dissolution of adsorbed tight oil is 2.498 g/cm^3~2.682 g/cm^3, with an average of 2.584 g/cm^3. After Soxhlet extraction, the rock density is 2.247 g/cm^3~2.348 g/cm^3, with an average of 2.294 g/cm^3, related to the continuous dissolution of adsorbed tight oil in the reservoir and the increased storage space (Figure 6).

5.2. Effect of Adsorbed Tight Oil on the Changes of Porosity and Permeability. The relationship between adsorbed tight oil and porosity and permeability changes of the Chang 8 tight reservoir has been analyzed (Figure 7). The porosity of six samples increased by 2.07%~5.47%, and the average porosity increased by 3.14% after Soxhlet extraction (Figure 7(a)). The permeability changes are increased by
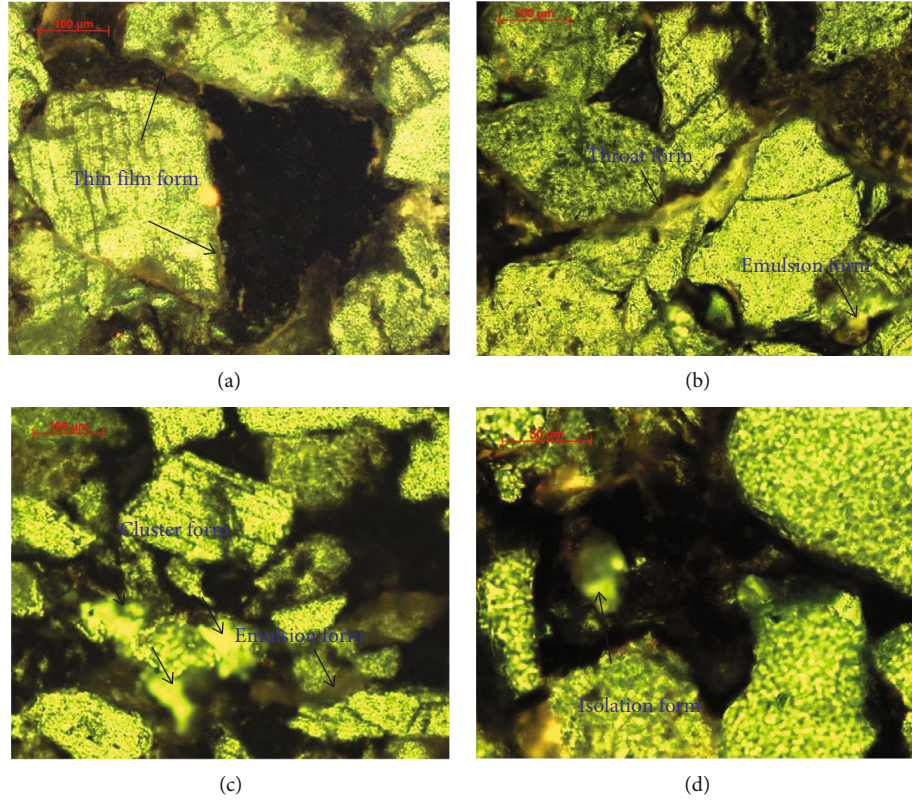
FIGURE 5: Classification of the absorbed tight oil occurrence forms. (a) Chlorite and iron calcite surface absorbed thin film form oil (B280-13-3). (b) Throat form in throat and cluster form in cements (B436-7-33). (c) Emulsion form in interparticle pore and cluster forms in feldspar dissolved pore (B455-2-60). (d) Isolation form in the intracystalline pore (B456-6-06).

TABLE 3: Data of rock density and porosity permeability change before and after Soxhlet extraction.

Samples	Depths (m)	Φ_{before} (%)	K_{before} ($\times10^{-3}\,\mu m^2$)	D_{before} (g/cm^3)	Φ_{after} (%)	K_{after} ($\times10^{-3}\,\mu m^2$)	D_{after} (g/cm^3)	$\triangle\Phi$/%	$\triangle K/\times10^{-3}\,\mu m^2$	$\triangle\Phi\%$/%	$\triangle K\%$/%
B455-2-46	2147.87	18.10	8.850	2.682	23.57	9.338	2.251	5.47	0.488	23.21	5.23
B455-2-60	2149.47	13.36	2.327	2.664	16.63	2.901	2.247	3.27	0.574	19.66	19.79
B436-7-33	2192.60	9.41	0.349	2.534	12.03	0.584	2.348	2.62	0.235	21.78	40.24
B436-7-38	2193.20	10.69	0.493	2.588	13.38	0.827	2.306	2.69	0.334	20.10	40.39
B456-6-6	2134.20	11.61	0.474	2.536	14.35	0.639	2.314	2.74	0.165	19.09	25.82
B280-13-3	2213.35	10.95	0.114	2.498	13.02	0.244	2.296	2.07	0.130	15.90	53.28

$0.13 \times 10^{-3}\,\mu m^2 \sim 0.574 \times 10^{-3}\,\mu m^2$ with an average of $0.321 \times 10^{-3}\,\mu m^2$ (Figure 7(b)). The numerical variation is not obvious. However, by comparing the changing rates of porosity ($\triangle\varphi\%$) and permeability ($\triangle K\%$), after Soxhlet extraction, the changing rates of porosity and permeability are 15.90%~23.21% (with an average of 19.96%) and 5.23~53.28% (with an average of 30.79%), respectively (Figures 7(c) and 7(d) and Table 3). These results may be related to the fact that previous studies only pay attention

to the proportion of storage space in the reservoir but not to the connected pores before and after Soxhlet extraction. The experimental results show that all kinds of adsorbed oil can be dissolved. The tight oil adsorbed in the throat is more dissolved than the tight oil adsorbed in the pores. Because of the existence of grain-coating chlorite, the adsorption between adsorbed tight oil and chlorite is stronger, which made it more difficult to dissolve the adsorbed tight oil in the pore, especially the pore with grain-coating
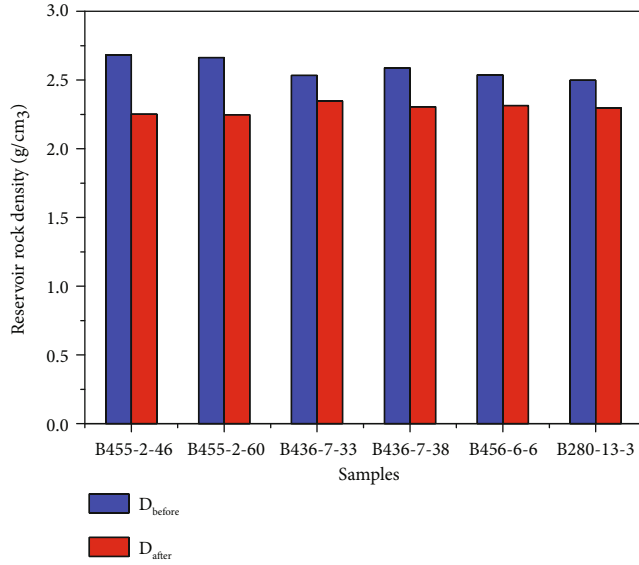
FIGURE 6: Variation of rock density before and after Soxhlet extraction.

chlorite development. These results show that the tight oil adsorbed on the surface of the clay is more difficult to be separated (Figures 2(d)–2(f)).

In comparison, for the samples with better initial porosity and permeability (B455-2-46), its porosity and permeability change rates are 23.21% and 5.23%, respectively; for the samples with worse initial porosity and permeability (B280-13-3), its porosity and permeability change rates are 15.90% and 53.28%, respectively. The results show that the initial physical properties of the reservoir may have a significant impact on the separation process of tight oil. The connectivity difference of the pore throat may be one of the reasons for the change of porosity and permeability. However, in higher densification degree reservoirs, the porosity and permeability change rates grow more obviously. These results show that tight oil's adsorption process in the reservoir leads to reservoir densification.

5.3. Effect of Pore Structure Types on the Adsorbed Tight Oil. The throat is the relatively narrow part between the connected pores. And the shape and size of the throat directly affect the connectivity of the pores and thus affect the behavior of the form adsorbed tight oil. Six samples were tested by high-pressure mercury injection (HPMI) after Soxhlet extraction. According to the pore structure parameters obtained from high-pressure mercury injection, the shape of capillary force curve, the pore structure was divided into four types. Combined with the occurrence morphology of adsorbed tight oil in samples with different pore structures, different pore structures have different main types and different contents of adsorbed tight oil. In the process of Soxhlet extraction to dissolve the adsorbed tight oil, different types of the adsorbed form may have different dissolved degrees: emulsion form, which mainly occurs in interparticle pore, and throat form, which mainly occurs in the throat, are accessible to be dissolved; cluster form which mainly occurs

in the dissolved pore and the edge of cement is hard to dissolve; isolation form which mainly occurs in intracrystalline pore is the hardest to be dissolved (because organic reagents are difficult to enter the intercrystalline pores during extraction process); thin film form which occurs in particle surface has a significant difference in the adsorption capacity according to the mineral properties [21, 23, 28–30, 45].

The relationship between adsorption tight oil types and the change of porosity permeability before and after Soxhlet extraction has been studied (Figure 8). The results show that emulsion form, cluster form, and throat form have a positive correlation with the change of porosity and permeability (Figures 8(a)–8(c) and 8(f)–8(h)), but for thin film form, isolation form has a negative correlation with the change of porosity and permeability (Figures 8(d) and 8(e) and 8(i) and 8(j)). The relationship of adsorbed tight oil (emulsion form, cluster form, and throat form) with permeability change ($R^2 = 0.692$, $R^2 = 0.640$, and $R^2 = 0.759$, respectively) is more substantial than that with porosity change ($R^2 = 0.634$, $R^2 = 0.574$, and $R^2 = 0.562$, respectively). With the initial permeability of samples increasing, the porosity and permeability increase obviously after Soxhlet extraction. In comparison, the reservoir's adsorbed tight oil occurrence characteristics (emulsion form, cluster form, and throat form) are more sensitive to permeability than to porosity. This phenomenon may be related to the porosity representing reservoir space's capacity, while permeability represents the interconnected pore in the reservoir. Therefore, these analyses indicate that under Soxhlet extraction, the adsorbed tight oil (emulsion form, cluster form, and throat form) in the reservoir controls by the connectivity of the pores. The relationship of adsorbed tight oil (thin film form and isolation form) with permeability change ($R^2 = 0.742$ and $R^2 = 0.686$, respectively) is more vital than that with porosity change ($R^2 = 0.763$ and $R^2 = 0.246$, respectively). This result shows that the thin-film and isolated adsorption states developed on the surface of clay minerals and in intergranular pores are more challenging to be desorbed. This phenomenon is related to the strong adsorption capacity of clay minerals for crude oil. This behavior indicates that different absorbed tight oil types have different dissolved efficiently under Soxhlet extraction. The emulsion, cluster, and throat forms are easier to dissolve, but thin film forms and isolation are harder to dissolve under Soxhlet extraction.

According to the relationships of the adsorbed tight oil types of the Chang 8 reservoir and of the four types of pore structure with the porosity and permeability, the difference of pore structure controls the distribution characteristics of pore throat, affects the physical properties of the reservoir, and then controls the distribution of adsorbed tight oil in the reservoir. Based on the correlation between the adsorbed tight oil types (the adsorption capacity) and the pore structure of samples, the relationship between pore structure type and porosity permeability before and after Soxhlet extraction is expressed as follows. The type A pore structure sample is B455-2-46, with a porosity change of 5.47%, a change rate of 23.21%, and a permeability change of $0.488 \times 10^{-3} \, \mu m^2$, with a change rate of 5.26%. The type B of pore structure sample
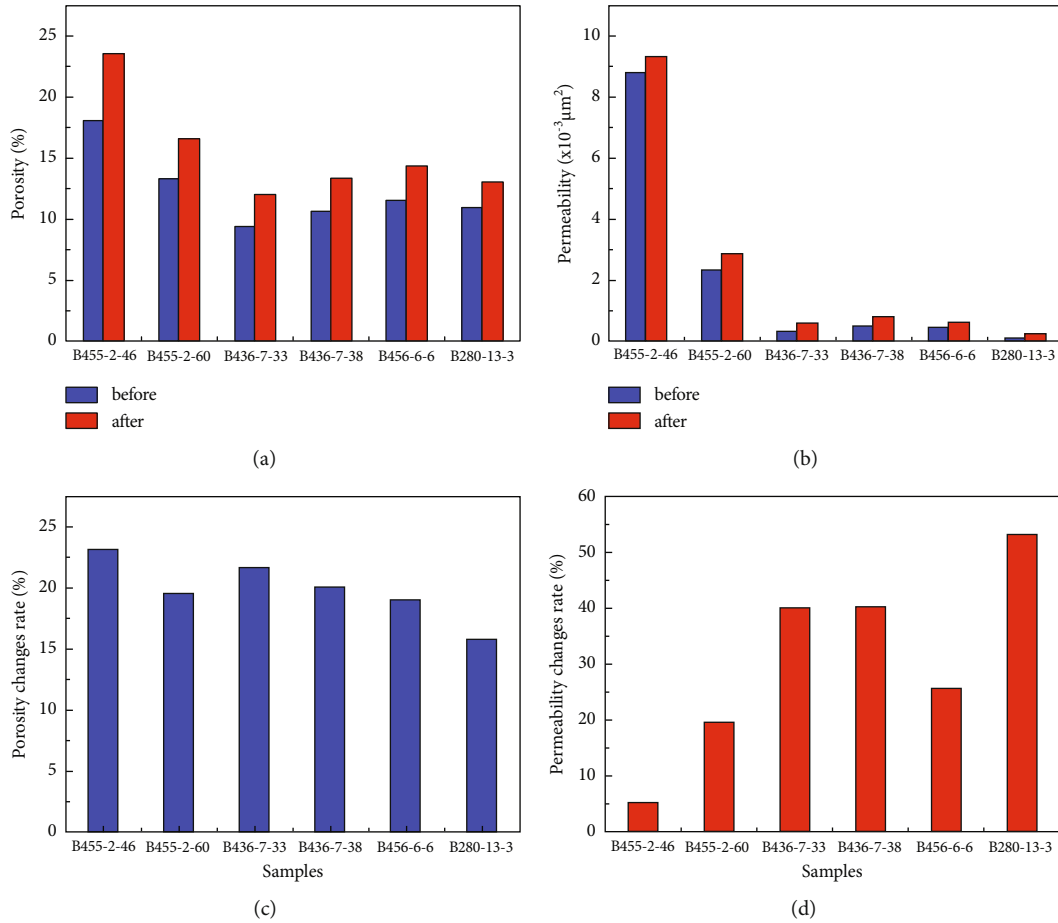
FIGURE 7: Changes of reservoir porosity and permeability before and after Soxhlet extraction. (a) Porosity changes. (b) Permeability changes. (c) Porosity change rate. (d) Permeability change rate.
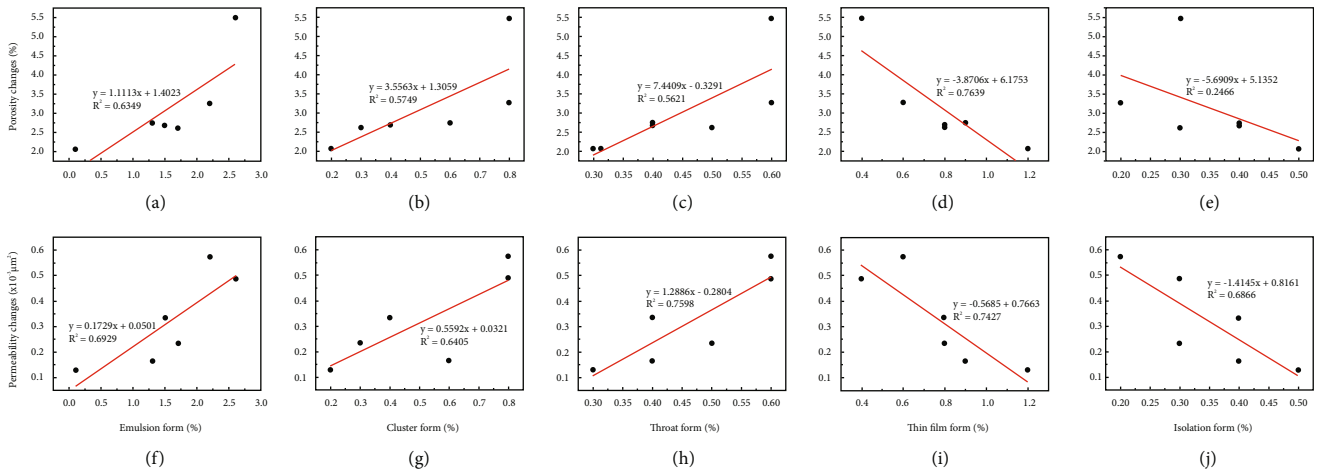

FIGURE 8: The relationship between adsorption tight oil types and the change of porosity permeability before and after Soxhlet extraction. (a–e) The relationship of emulsion form, cluster form, throat form, thin film form, and isolation form with the change of porosity before and after Soxhlet extraction; (f–j) the relationship of emulsion form, cluster form, throat form, thin film form, and isolation form with the change of permeability before and after Soxhlet extraction.

is B455-2-60, with a porosity change of 3.27%, a change rate of 19.66%, and a permeability change of $0.574 \times 10^{-3} \mu m^2$, with a change rate of 19.79%. The type C of pore structure samples is B436-7-33, B436-7-38, and B456-6-6, the varia-

tion of porosity is 2.62%~2.74%, the average variation is 2.68%, and the average variable rate is 20.33%. The variation of permeability is $0.165 \times 10^{-3} \mu m^2$~$0.344 \times 10^{-3} \mu m^2$, the average variation is $0.245 \times 10^{-3} \mu m^2$, and the average
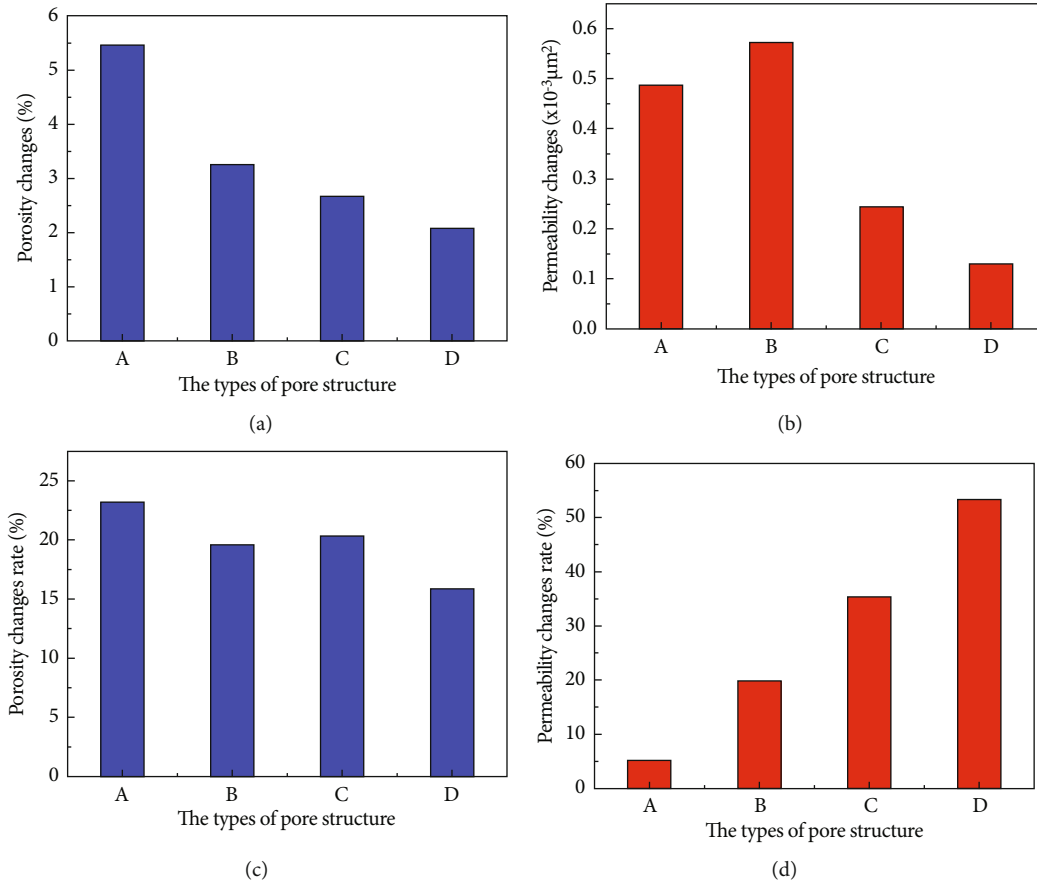
(a)

(b)

(c)

(d)

FIGURE 9: The relationship between pore structure types and porosity permeability before and after Soxhlet extraction. (a) Pore structure type and porosity changes. (b) Pore structure type and permeability changes. (c) Pore structure type and porosity change rate. (d) Pore structure type and permeability change rate.

variable rate is 35.48%. The type D of pore structure sample is B280-13-3, with a porosity change of 2.07%, a change rate of 15.9%, and a permeability change of $0.13 \times 10^{-3} \, \mu m^2$, with a change rate of 53.28%. The variation of porosity and permeability shows a decreasing trend (Figures 9(a) and 9(b)). It shows that the better the pore structure, the more substantial the reservoir capacity, and the more adsorbed the oil content. After Soxhlet extraction, the space occupied by adsorbed tight oil in the reservoir can release, and the reservoir conditions are improved. The larger the reservoir space is, the more the adsorption capacity of tight oil is. The higher the dissolution ratio of adsorbed tight oil after Soxhlet extraction is, the better the reservoir improvement effect is. Before and after Soxhlet extraction, the changing rates of porosity and permeability and pore structure show a trend increasing with the change of pore structure (Figures 9(c) and 9(d)), indicating that the more compact the reservoir, the more complex the pore structure is, and the stronger the damage of adsorbed tight oil to reservoir capacity, especially the damage of adsorbed tight oil to seepage capacity of tight reservoir which deserves attention. Therefore, for low permeability tight sandstone reservoirs, it is more important to work on the effect of tight oil adsorption on physical properties and pore structure.

5.4. Effect of Minerals on the Absorbed Tight Oil. Because of the influence of minerals on reservoir performance, predecessors mainly focused on the correlation between minerals and pore permeability of reservoirs to discuss their control on reservoir performance [46–48]. This study proposes that the types and contents of skeleton minerals such as quartz feldspar and authigenic minerals (mainly clay minerals) control the reservoir performance by tight oil adsorption.

The adsorbed tight oil in the interparticle pore surrounded by quartz and feldspar grains mainly has emulsion from adsorbed tight oil. Feldspar dissolved pore has cluster form adsorbed tight oil in the dissolved pore. Intracrystalline pore has isolation form adsorbed tight oil. Quartz and feldspar have a particular adsorptive ability to tight oil, and they can form thin film tight oil adsorbing layer on the surface of mineral particles. Clay minerals have a robust adsorptive ability to tight oil. The clay minerals of Chang 8 reservoir in the Huaqing area are mainly chlorite, primarily associated with grain-coating chlorite. The tight oil adsorption layer adsorbed on its surface is primarily thin film form.

The mineral composition of reservoirs correlates with absorbed tight oil of types (Figure 10). Quartz content is positively correlated with emulsion form and throat form but negatively correlated with cluster form, thin film form,
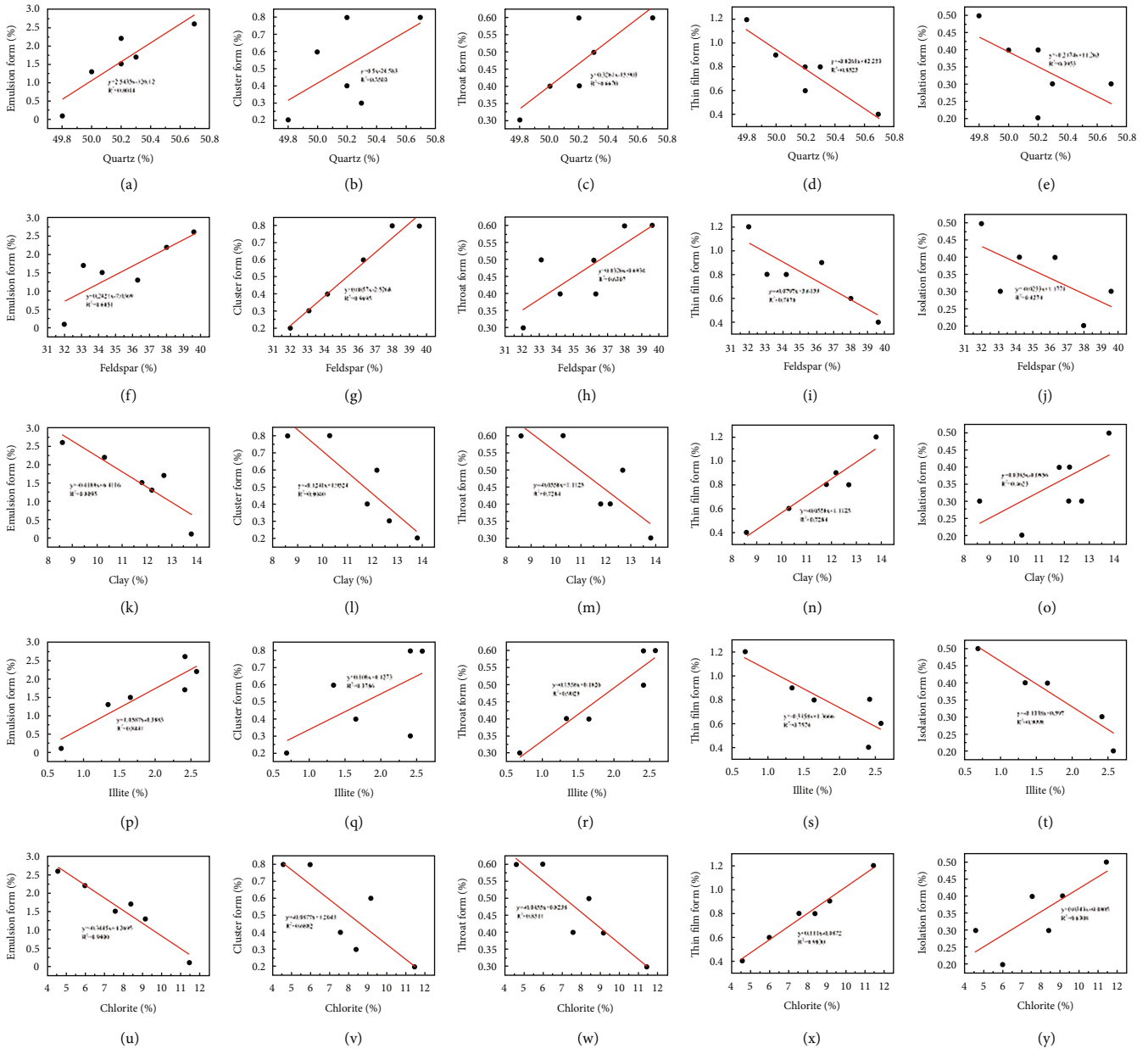
FIGURE 10: The relationship between adsorption tight oil types and minerals. (a–e) Quartz; (f–j) feldspar; (k–o) clay; (p–t) illite; (u–y) chlorite.

and isolation form of absorbed tight oil microoccurrence morphology (Figures 10(a)–10(e)). These results may be related to the higher the quartz content, the better the reservoir pore permeability and the interparticle pore and throat development. Feldspar content is positively correlated with emulsion form and cluster form but negatively correlated with throat form, thin film form, and isolation form of absorbed tight oil microoccurrence morphology (Figures 10(f)–10(j)). This phenomenon may be related to the dissolution of feldspar and the development of dissolved pores during oil and gas filling. Clay mineral content is positively correlated with thin film form and isolation form but negatively correlated with throat form, emulsion form, and cluster form of absorbed tight oil microoccurrence morphology (Figures 10(k)–10(o)). This phenomenon shows that the clay minerals control thin-film

distribution and isolated tight oil in the reservoir. Illite content is positively correlated with emulsion form and throat form but negatively correlated with cluster form, thin film form, and isolation form of absorbed tight oil microoccurrence morphology (Figures 10(p)–10(t)). The growth of illite requires an interconnected pore and throat to bring formation water in and out. These results mean the initial pore and permeability, the pore-throat connectivity is advantageous, and this trend is related. Chlorite content is positively correlated with thin film form and isolation form but negatively correlated with throat form, emulsion form, and cluster form of absorbed tight oil occurrence morphology (Figures 10(u)–10(y)). This result is similar to clay minerals and may be related to the fact that chlorite is the main clay mineral in the study area, and chlorite has a strong adsorption capacity for tight oil.
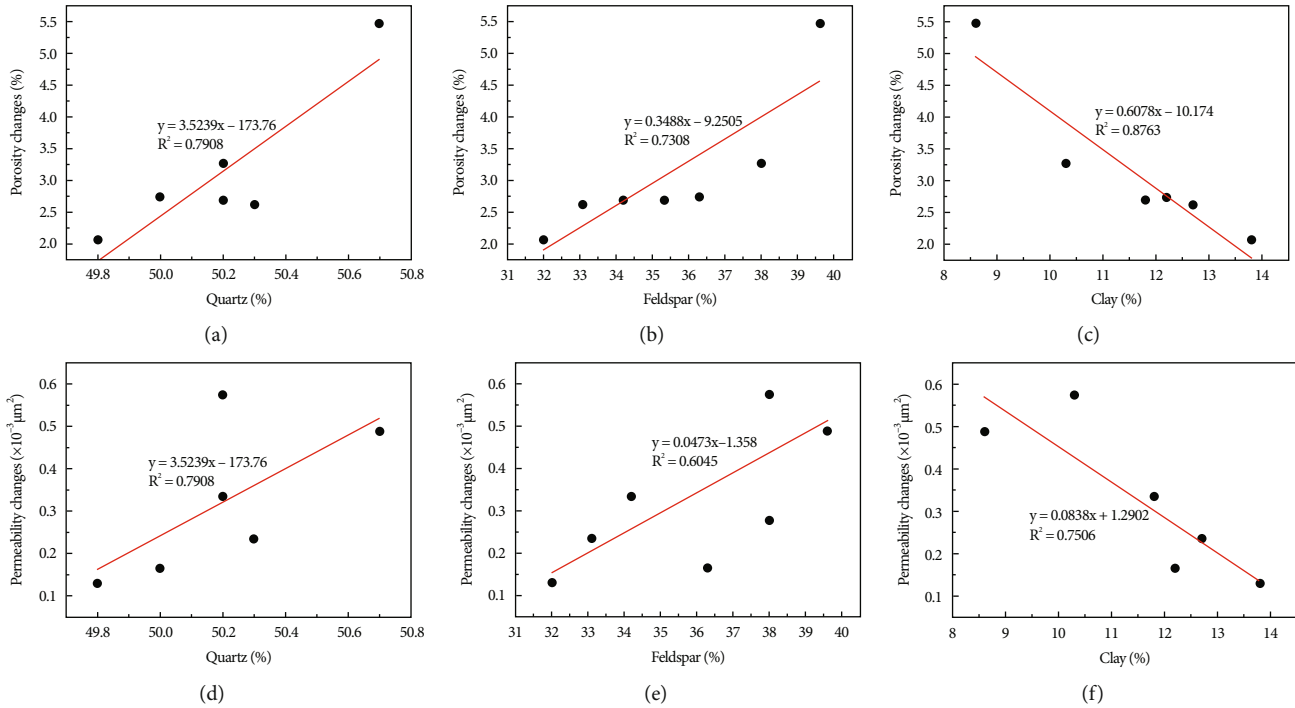
FIGURE 11: Relationship between quartz, feldspar, and clay content with the changes of porosity and permeability. (a–c) The content of quartz, feldspar, and clay with the porosity changes, respectively; (d–f) the content of quartz, feldspar, and clay with the permeability changes, respectively.

The variation of porosity and permeability is positively correlated with the content of quartz and feldspar (Figures 11(a) and 11(b) and 11(d) and 11(e)). One reason for that is the higher the content of quartz and feldspar, the more the interparticle pores developed and the higher reservoir space led to the higher adsorbed tight oil content. The other reason is that the higher the content of quartz feldspar is, the weaker the adsorption capacity of minerals surface to tight oil [23, 24]. During Soxhlet extraction, the adsorbed tight oil is more easily dissolved by organic reagents, which lead to the higher the content of quartz and feldspar, the more significant changes of porosity and permeability before and after Soxhlet extraction. But the total amount of clay minerals is negatively correlated with the change of porosity and permeability (Figures 11(c) and 11(f)). This phenomenon shows that grain-coating chlorite can partition the pore water on the mineral surface, inhibit the overgrowth of quartz and other minerals, increase the mechanical strength and compaction resistance of sandstone, and is conducive to the preservation of particular primary pore [49]. When the chlorite content is too high (>6%~7%), the pore and permeability space decrease, resulting in poor reservoir physical properties [50]. The clay mineral content of Chang 8 reservoir in the Huaqing area is of averaged 11.57%, and the chlorite content ranged from 4.558% to 11.454%, with an average of 7.845%, which destroyed the physical properties. In addition, during the initial filling process, the adsorption layer formed by the interaction between polar components and clay minerals in tight oil further destroyed the reservoir quality. Chlorite and illite have strong adsorption to tight oil, much larger

than the adsorption capacity of quartz for tight oil [23, 24]. Therefore, the adsorption capacity will increase with the clay mineral content. However, with the increase of clay mineral content, the physical properties of the reservoir are damaged, resulting in relatively small changes in porosity and permeability. In addition, due to the strong interaction between clay minerals and dense oil, the dense oil adsorbed on the surface of clay minerals is not easy to dissolve by organic reagents in Soxhlet extraction. With the increase of clay mineral content, it is hard to dissolve organic reagents in the adsorbed tight oil content. In addition, the higher the clay mineral, the apparent negative correlation between the total mineral content and porosity and permeability change. Therefore, evaluating porosity and permeability change is essential based on reservoirs' mineral types and contents.

5.5. Effect of Clay Minerals on Absorbed Tight Oil. To determine the influence of clay mineral types and content on the porosity permeability change, one should know tight oil's clay mineral adsorption capacity. The chemical composition of adsorbed tight oil and its occurrence characteristics in reservoirs play an essential role in determining the stability of tight oil adsorption on reservoir damage. Regarding the interaction between tight oil and clay minerals, the amount of adsorbed tight oil and selecting an appropriate displacement method maybe play an essential role in developing reservoir [23].

The clay minerals in Chang 8 reservoir are widely distributed and varied, accounting for 11.57%. The X-ray diffraction analysis shows that chlorite and illite accounted
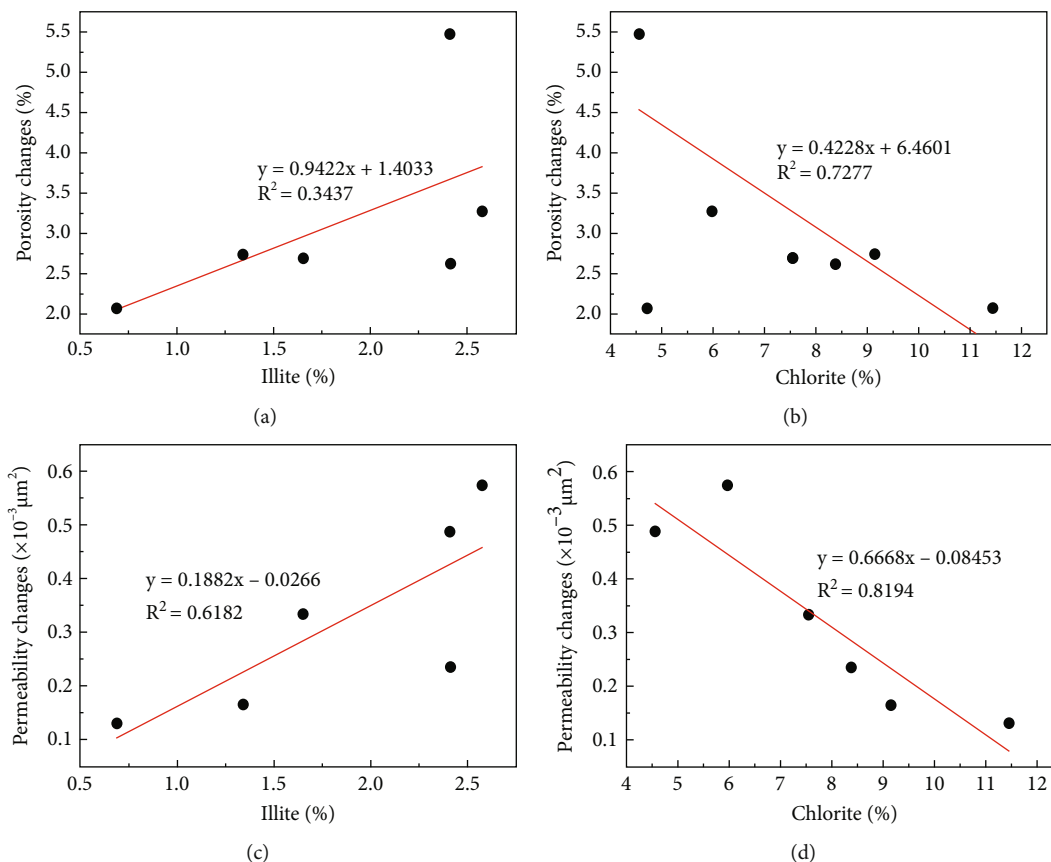
FIGURE 12: (a) Relationship between illite content and porosity changes. (b) Relationship between chlorite content and porosity changes. (c) Relationship between illite content and permeability changes. (d) Relationship between chlorite content and permeability changes.

for 7.845% and 1.85%, respectively. The illite content with porosity permeability change rate shows a positive correlation (Figures 12(a) and 12(c)), and chlorite content with porosity permeability change shows a negative correlation (Figures 12(b) and 12(d)).

Illite fills the interparticle pore with hair-like aggregates and fibers, which could plug the pore throat and make the effective pore become invalid micropore quickly, thus significantly reducing the permeability of the reservoir. However, illite occurs nearly in the middle of the pore with hair and fiber, enlarging the specific surface area to absorb tight oil. Considering that the development of illite is mainly concentrated in the middle of the pore throat, organic matters will be preferentially affected when flowing in the pore throat. Therefore, the porosity and permeability of the reservoir will increase with the dissolution of tight oil adsorbed by illite (Figures 12(a) and 12(c)). The samples with high illite content have relatively good physical properties and relatively strong percolation ability. In the Soxhlet extraction process, the organic reagents and adsorbed tight oil are more sufficiently effective and soluble. Chlorite occurs mainly in the form of particle film covering. Scanning electron microscopy shows that chlorite occurs in an approximate ring of equal thickness with a thickness of about 8-12 μm, surrounded by mineral particles. Black adsorbed tight oil encapsulation can be seen in fluorescent and casting slices due to chlorite and tight oil during oil and gas filling. The considerable

thickness of the adsorption layer could result in the blockage of the pore throat. This phenomenon is related to the fact that tight oil adsorbed on the surface of chlorite is seldom dissolved due to it is near the edge of the pore throat and is less affected by organic reagents. Therefore, there is a negative correlation between chlorite content and porosity and permeability changes. In addition, the growth of authigenic chlorite may change the microflow in oil and gas filling, which is also one of the reasons for this phenomenon. In addition, chlorite improves adsorption capacity and can promote the precipitation of asphaltene with sufficient oil and gas filling. The tight sandstones with higher illite should be targeted rather than those with higher chlorite content while exploring adsorbed tight oil.

6. Conclusion

Fluorescence thin sections and field emission scanning electron microscopy observation, high-pressure mercury intrusion method, X-ray diffraction, and porosity and permeability measurements were employed to obtain the pore structure, mineral composition, pore throat size distribution, and the distribution of adsorbed tight oil of mixture samples including different pore structures to illustrate the occurrence characteristics and its effects of porosity and permeability reduction of tight sandstones. The following conclusions were reached:

(1) Adsorbed tight oil is widely distributed in the residual interparticle pore, dissolved pore, intercrystalline pore, and mineral surfaces of tight sandstone reservoirs. And it is primarily concentrated in the pore – throat radius < $0.25\,\mu$m

(2) The development shape and size of the reservoir control the distribution of the adsorbed tight oil. According to the differences in occurrence location, morphology, and fluorescence color, the adsorbed tight oil is divided into five types: emulsion form, cluster form, throat form, thin film form, and isolation form, which are mainly stored in interparticle pores, feldspar dissolved pores, throats, the surface of minerals, and intercrystalline pores, respectively

(3) The adsorption of tight oil in the reservoir results in tight sandstone reservoirs' pore and throat reduction. And it is one of the reasons for reservoir densification. The adsorption of tight oil in the reservoir leads to increased reservoir density by $0.290\,\mathrm{g/cm^3}$ and the reduction of porosity and permeability by 3.14% and $0.321 \times 10^{-3}\,\mu\mathrm{m^2}$, respectively. In addition, the permeability change rate by adsorbed tight oil is significantly more potent than that of porosity, which is 30.79% and 19.96%, respectively

(4) Adsorbed oil is a potential resource for enhanced oil recovery. The pore and throat reduction process of adsorbed tight oil is controlled by the size of reservoir space and the development of skeleton minerals and clay minerals, especially illite. In addition, the difference in the separation process of tight oil in different occurrence states is another critical reason to control the pore and throat reduction of tight oil. Reservoirs with large pore throat and low clay mineral content can be developed preferentially in the development process

Data Availability

All data included in this study are available upon request by contact with the corresponding author.

Conflicts of Interest

The authors declare that they have no conflicts of interest.

Acknowledgments

References

[1] J. L. Clayton and P. J. Swetland, "Petroleum generation and migration in Denver basin," *American Association of Petroleum Geologists Bulletin*, vol. 64, pp. 1613–1633, 1980.

[2] S. M. Landon, M. W. Longman, and B. A. Luneau, "Hydrocarbon source rock potential of the Upper Cretaceous Niobrara Formation, Western Interior Seaway of the Rocky Mountain region," *Mountain Geologist*, vol. 1, pp. 1–18, 2001.

[3] P. P. Kuhn, R. D. Primio, R. Hill, J. R. Lawrence, and B. Horsfield, "Three-dimensional modeling study of the low-permeability petroleum system of the Bakken Formation," *AAPG Bulletin*, vol. 96, no. 10, pp. 1867–1897, 2012.

[4] A. S. Sonnenberg and A. Pramudito, "Petroleum geology of the giant Elm Coulee field, Williston Basin," *AAPG Bulletin*, vol. 93, no. 9, pp. 1127–1153, 2009.

[5] J. A. LeFever, R. D. LeFever, and S. H. Nordeng, "Reservoirs of the Bakken Petroleum System: a core-based perspective," 2013, Search and Discovery Article #10535.

[6] T. F. Hentz, W. A. Ambrose, and D. C. Smith, "Eaglebine play of the southwestern East Texas basin: stratigraphic and depositional framework of the Upper Cretaceous (Cenomanian-Turonian) Woodbine and Eagle Ford Groups," *AAPG Bulletin*, vol. 98, pp. 2551–2580, 2014.

[7] R. A. Denne, R. E. Hinote, J. A. Breyer et al., "The Cenomanian-Turonian Eagle Ford Group of South Texas: insights on timing and paleoceanographic conditions from geochemistry and micropaleontologic analyses," *Palaeogeography*, vol. 413, pp. 2–28, 2014.

[8] B. Alotaibi, D. Schechter, and R. A. Wattenbarger, "Production forecast, analysis and simulation of Eagle Ford Shale oil wells," in *SPE Middle East Unconventional Resources Conference and Exhibition*, Muscat, Oman, 2015.

[9] A. S. Sonnenberg, "The Giant Continuous Oil Accumulation in the Bakken Petroleum System, Williston Basin," in *Giant Fields of the Decade 2000–2010*, pp. 1–10, AAPG Search and Discovery, 2015.

[10] M. D. Fairbanks, S. C. Ruppel, and H. Rowe, "High-resolution stratigraphy and facies architecture of the Upper Cretaceous (Cenomanian–Turonian) Eagle Ford Group, Central Texas," *AAPG Bulletin*, vol. 100, no. 3, pp. 379–403, 2016.

[11] S. T. Wu, C. N. Zou, R. K. Zhu et al., "Characteristics and origin of tight oil accumulations in the Upper Triassic Yanchang Formation of the Ordos Basin, North-Central China," *Acta Geologica Sinica*, vol. 90, no. 5, pp. 1821–1837, 2016.

[12] S. A. Sonnenberg, "The Niobrara Petroleum System: a new resource play in the Rocky Mountain Region," in *Revisiting and Revitalizing the Niobrara in the Central Rockies*, J. E. Estes-Jackson and D. S. Anderson, Eds., pp. 1–32, Rocky Mountain Association of Geologists, Denver, Colo, 2011.

[13] S. A. Sonnenberg, *Keys to Niobrara and Codell Production, East Pony/Redtail Area*, AAPG Search and Discovery Article, Denver Basin, Colorado, 2017.

[14] F. Jinhua, *Theory and Technology of Tight Oil Exploration in Ordos Basin*, Science Press, 2018.

[15] L. Bai, B. Liu, J. Yang, S. Tian, B. Wang, and S. Huang, "Differences in hydrocarbon composition of shale oils in different phase states from the Qingshankou Formation, Songliao Basin, as determined from fluorescence experiments," *Frontiers of Earth Science*, vol. 15, no. 2, pp. 438–456, 2021.

[16] L. Bai, B. Liu, and Y. Du, "Distribution characteristics and oil mobility thresholds in lacustrine shale reservoir: insights from N_2 adsorption experiments on samples prior to and following hydrocarbon extraction," *Petroleum Science*, 2021.

[17] B. J. Marlow, G. C. Sresty, R. D. Hughes, and O. P. Mahajan, "Colloidal stabilization of clays by asphaltenes in hydrocarbon media," *Colloids surf*, vol. 24, no. 4, pp. 283–297, 1987.

[18] A. Saada, B. Siffert, and E. J. Papirer, "Comparison of the hydrophilicity/hydrophobicity of illites and kaolinites," *Colloid Interface Sciences*, vol. 174, no. 1, pp. 185–190, 1995.

[19] G. Piro, L. Barberis Canonico, G. Galbariggi, L. Bertero, and C. Carniani, "Asphaltene adsorption onto formation rock: an approach to asphaltene formation damage prevention," *SPE Journal*, vol. 11, no. 3, pp. 156–160, 1996.

[20] H. Gaboriau and A. Saada, "Influence of heavy organic pollutants of anthropic origin on PAH retention by kaolinite," *Chemosphere*, vol. 44, no. 7, pp. 1633–1639, 2001.

[21] A. W. Marczewski and M. Szymula, "Adsorption of asphaltenes from toluene on mineral surface," *Colloids surf A*, vol. 208, no. 1-3, pp. 259–266, 2002.

[22] G. Gonzalez and A. Middea, "Peptization of asphaltene by various oil soluble amphiphiles," *Colloids surf A*, vol. 52, pp. 207–217, 1991.

[23] T. Pernyeszi, A. Patzko, O. Berkesi, and I. Dekany, "Asphaltene adsorption on clays and crude oil reservoir rocks," *Colloids surf A*, vol. 137, no. 1-3, pp. 373–384, 1998.

[24] T. Pernyeszi and I. Dekany, "Sorption and elution of asphaltenes from porous silica surfaces," *Colloids surf A*, vol. 194, no. 1-3, pp. 25–39, 2001.

[25] C. Drummond and J. Israelachvili, "Fundamental studies of crude oil-surface water interactions and its relationship to reservoir wettability," *Journal of Petroleum Science and Engineering*, vol. 45, no. 1-2, pp. 61–81, 2004.

[26] K. Kumar, E. Dao, and K. K. Mohanty, "AFM study of mineral wettability with reservoir oils," *Journal of Colloid and Interface Science*, vol. 289, no. 1, pp. 206–217, 2005.

[27] W. A. Abdallah and S. D. Taylor, "Surface characterization of adsorbed asphaltene on a stainless steel surface," *Nuclear Instruments and Methods in Physics Research Section B: Beam Interactions with Materials and Atoms*, vol. 258, no. 1, pp. 213–217, 2007.

[28] V. Gonzalez and S. E. Taylor, "Asphaltene adsorption on quartz sand in the presence of pre-adsorbed water," *Journal of Colloid and Interface Science*, vol. 480, pp. 137–145, 2016.

[29] S. Wang, Q. Liu, X. Tan, C. Xu, and M. R. Gray, "Adsorption of asphaltenes on kaolinite as an irreversible process," *Colloids and Surfaces A: Physicochemical and Engineering Aspects*, vol. 504, pp. 280–286, 2016.

[30] F. E. Pinto, E. V. Barros, L. V. Tose et al., "Fractionation of asphaltenes in _n_ -hexane and on adsorption onto $CaCO_3$ and characterization by ESI(+)FT-ICR MS: part I," *Fuel*, vol. 210, pp. 790–802, 2017.

[31] W. Minglei, Z. Sui'an, and Z. Fudong, "Quantitative research on tight oil microscopic state of Chang 7 Member of Triassic Yanchang Formation in Ordos Basin, NW China," *Petroleum Exploration and Development*, vol. 42, no. 6, pp. 827–832, 2015.

[32] G. Yanjie, L. Shaobo, and Z. Rukai, "Micro-occurrence of Cretaceous tight oil in southern Songliao Basin, NE China," *Petroleum Exploration and Development*, vol. 42, no. 3, pp. 323–328, 2015.

[33] H. Zhao Wenzhi and W. Z. Suyun, "Key role of basement fault control on oil accumulation of Yanchang Formation, Upper Triassic, Ordos Basin," *Petroleum Exploration and Development*, vol. 30, no. 5, pp. 1–5, 2003.

[34] Y. Hua and Z. Wenzheng, "Leading effect of the seventh member high-quality source rock of Yanchang Formation in Ordos basin during the enrichment of low-penetrating oil-gas accumulation—geology and geochemistry," *Geochemica*, vol. 37, no. 1, pp. 59–64, 2005.

[35] Z. Wenzheng, Y. Hua, and L. Jianfeng, "Leading effect of the seventh member high-quality source rock of Yanchang Formation in Ordos basin during the enrichment of low-penetrating oil-gas accumulation—hydrocarbon generation and expulsion mechanism," *PetroleumExploration and Development*, vol. 33, no. 3, pp. 289–293, 2006.

[36] Z. Caineng, Z. Rukai, and B. Bin, "First discovery of nanopore throat in oil and gas reservoir in China and its scientific value," *Acta Petrologica Sinica*, vol. 27, no. 6, pp. 1857–1864, 2011.

[37] C. Zou, R. Zhu, K. Liu et al., "Tight gas sandstone reservoirs in China: characteristics and recognition criteria," *Journal of Petroleum Science and Engineering*, vol. 88-89, pp. 82–91, 2012.

[38] M. Wangcai, M. Xiangzhen, and C. Lijun, "Assessment of tight oil resources in the Chang 6-Chang 9 sections of Yanchang Formation from the Ordos Basin," *China Energy and Environmental Protection*, vol. 11, 2018.

[39] F. Shi Jinping and Z. X. Guomin, "Effect of adsorption of crude oil on fluid transfusion in low permeability reservoir," *Journal of Liaoning Technical University (Natural Scince)*, vol. 28, pp. 70–72, 2009.

[40] L. Peng, J. Chengzao, J. Zhijun, L. Quanyou, Z. Min, and H. Zhenkai, "The characteristics of movable fluid in the Triassic lacustrine tight oil reservoir: a case study of the Chang 7 member of Xin'anbian Block, Ordos Basin, China," *Marine and Petroleum Geology*, vol. 102, pp. 126–137, 2019.

[41] Z. Xiaomin, D. Xiuqin, and L. Ziliang, "Sedimentary characteristics and model of shallow braided delta in large-scale lacustrine: an example from Triassic Yanchang Formation in Ordos Basin," *Earth Sciscence Frontiers*, vol. 20, no. 2, 2013.

[42] S. H. Zhou, T. Zou, Q. S. Zhu, W. L. Huang, Y. Chen, and Y. Gao, *National Standard of People Republic of China: pore size distribution and porosity of solid material by mercury porosimetry and gas adsorption-part 1: mercury porosimetry*, Standards Press of China, Beijing, 2008.

[43] S. Wu, R. Zhu, Z. Yang, Z. Mao, C. Jingwei, and Z. Xiangxiang, "Distribution and characteristics of lacustrine tight oil reservoirs in China," *Journal of Asian earth sciences*, vol. 178, 2019.

[44] C. Shijia, Y. Jingli, and L. Jungang, "Reservoir bitumen genesis and its impacts on hydrocarbon migration and accumulation: a case study from Chang 81 of Yangchang Fomation in Huaqing area, the Ordos Basin," *Oil& Gas Geology*, vol. 33, no. 1, pp. 37–44, 2012.

[45] M. Szymula and A. W. Marczewski, "Adsorption of asphaltenes from toluene on typical soils of Lublin region," *Applied Surface Science*, vol. 196, no. 1-4, pp. 301–311, 2002.

[46] X. Runcheng, Z. Wen, and Y. Ningping, "Study on control factors of quality of compact sandstone reservoir-taking He8 formation of the Jingbian gas field as an example," *PETROLEUM GEOLOGY & EXPERIMENT*, vol. 32, no. 2, pp. 120–123, 2010.

[47] W. Fu Jing and S.,. F. Jiahua, "Reasearch on quantitative diage-netic facies of Yanchang Formation in Longdong Area," *Ordos Basin. Earth Science Frontiers*, vol. 70, no. 2, pp. 86–97, 2013.

[48] Z. Jizhi, C. Shijia, and X. Yan, "Characteristics of the Chang 8 tight sandstone reservoirs and their genesis in Huaqing area Ordos Basin," *OIL & GAS GEOLOGY*, vol. 34, no. 5, pp. 679–684, 2013.

[49] L. Yefang, H. SiJing, R. Liang, and Z. X. Hua, "Influence of authigenic chlorite on the relationship of porosity to perme-ability in the sandstone reservoir: a case study from Chang-8 oil-bearing formation of Triassic in Jiyuan-Huaqing area, Ordos Basin," *JOURNAL OF CHENGDU UNIVERSITY OF TECHNOLOGY (Science & Technology Edition)*, vol. 38, no. 3, pp. 313–320, 2011.

[50] Z. Xi, S. Wei, and R. Dazhong, "Quantitative calculation of porosity evolution and formation mechanism of tight sand-stone in Chang 63 reservoirs of the Huaqing area, Ordos basin," *Geology and Exploration*, vol. 53, no. 4, pp. 807–817, 2017.